Available online at www.sciencedirect.com
SCIENCE DIRECT®
Carbohydrate Research 339 (2004) 825–833
Carbohydrate RESEARCH

Molecular and crystal structures of chitosan/HI type I salt determined by X-ray fiber diffraction

Amornrat Lertworasirikul,[a] Shingo Yokoyama,[a] Keiichi Noguchi,[b] Kozo Ogawa[c] and Kenji Okuyama[a,*]

[a]*Faculty of Technology, Tokyo University of Agriculture and Technology, Koganei, Tokyo 184-8588, Japan*
[b]*Instrumentation Analysis Center, Tokyo University of Agriculture and Technology, Koganei, Tokyo 184-8588, Japan*
[c]*Research Institute for Advanced Science and Technology, Osaka Prefecture University, Sakai, Osaka 599-8570, Japan*

Received 15 October 2003; accepted 6 January 2004

Abstract—The three-dimensional structure of chitosan/HI type I salt was determined by the X-ray fiber diffraction technique and linked-atom least-squares refinement method. Two polymer chains and four iodide ions (I^-) crystallized in a monoclinic unit cell with dimensions $a = 9.46(2)$, $b = 9.79(2)$, c (fiber axis) $= 10.33(2)$ Å, $\beta = 105.1(2)°$ and a space group $P2_1$. Chitosan chains adopted an extended twofold helical conformation that was stabilized by O-3···O-5 hydrogen bonds, and the O-6 atom adopted nearly *gt* orientation. Polymer chains zigzag along the *b*-axis and directly connect to each other by N-2···O-6 hydrogen bonds. Two columns of iodide ions were shown to pack at the bending points of the zigzag sheets, and their locations are closely related to those of water columns in the hydrated chitosan. The iodide ions stabilized the salt structure by forming hydrogen bonds with the N-2 and O-6 atoms of the polymer chains together with an electrostatic interaction between N-2 and the iodide ions.

Keywords: Chitosan structure; Chitosan type I salt; Chitosan iodide salt; Fiber diffraction

1. Introduction

Chitosan, the N-deacetylated form of chitin, has been developed for diverse applications. The main driving force behind the development lies in the fact that this polysaccharide represents a renewable source of natural biodegradable polymers. Additionally, it has versatile properties such as biocompatibility[1–3] and nontoxicity,[4,5] as well as anti-bacterial,[6–8] anti-fungal,[9–11] anti-tumor,[12–14] metal-binding,[15–17] cholesterol-lowering,[18–21] and wound-healing[22,23] properties. More efficient development of the use of this polymer can be achieved if the structures of chitosan and its derivatives are elucidated.

The three-dimensional structure of chitosan has been studied by X-ray diffraction and electron diffraction.[24–27] So far, two crystalline forms of chitosan, hydrated,[24] and anhydrous,[25,28] have been found. The former is a deacetylated product of chitin and can be converted to the latter crystalline form by annealing[28] or transformation via chitosan/monocarboxylic salt.[29] Both crystalline forms have a conventional extended twofold helical conformation with an approximate 10-Å fiber repeat[24,25] that has been observed in other β-(1→4)-polysaccharides.[30,31] As for chitosan complexes, three types can be classified in accordance with their fiber repeat. The complexes with fiber repeats of about 10, 40, and 25 Å are called type I, type II, and type III, respectively. Chitosan/metal salt,[26] chitosan/HNO_3,[26,32] chitosan/HI,[32] chitosan/HBr,[32] and chitosan/ascorbic acid[33] were reported to be type I. Type II was observed in chitosan/monocarboxylic acids,[29,34] chitosan/HCl,[32,35] chitosan/HF,[32] and chitosan/H_2SO_4.[32] Type III was recently reported for chitosan/salicylic and chitosan/gentisic acids.[36]

Nevertheless, until recently, no detailed structure of any chitosan complex has been unveiled. In this study,

* Corresponding author. Tel./fax: +81-42-3887028; e-mail: okuya-mak@cc.tuat.ac.jp

0008-6215/$ - see front matter © 2004 Elsevier Ltd. All rights reserved.
doi:10.1016/j.carres.2004.01.001

we have analyzed the type I structure using synchrotron X-ray data collected from the chitosan/HI salt.

2. Structural analysis

2.1. Crystal data

The fiber diffraction pattern obtained by synchrotron radiation yields 44 independent spots up to the fifth layer line (Fig. 1). Those observed spots can be indexed as a monoclinic unit cell with the lattice parameters $a = 9.46(2)$, $b = 9.79(2)$, c (fiber axis) $= 10.33(2)$ Å and $\beta = 105.1(2)°$. Since systematic absences of odd reflections $(0k0)$ were observed, the space group was determined as $P2_1$.

Like chitosan,[24,25] the observed fiber period is about 10 Å. Therefore, the polymer chain in salt structure was presumed to have the extended 2/1-helical conformation. According to an observed density (1.98 g cm^{-3}) and a unit cell volume (957 Å^3), two polymer chains and four iodide ions (I^-) were accommodated in the unit cell without a water molecule (calculated density = 2.09 g cm^{-3}).

2.2. Molecular model building

A molecular model having 2/1-helical symmetry in the fiber period of 10.33 Å with a monosaccharide helical asymmetric unit was generated by using the WINLALS[37] program (Fig. 2). Standard geometry was obtained from the literature.[38] The conformation were defined by the conformational angles ϕ(C-2–C-1–O-1–C-4′) and ψ(C-1–O-1–C-4′–C-3′). These angles were fixed to the values that satisfied building conditions in the early stage of analysis and were refined in the final stage, together with the glycosidic linkage angle τ(C-1–O-1–C-4′). The orientation of the O-6 atom was defined by the dihedral angle χ(O-5–C-5–C-6–O-6). According to many related compounds, this angle fell into one of the following three orientations: *gauche–gauche* (*gg*, $\chi \approx -60°$), *gauche–trans* (*gt*, $\chi \approx 60°$) and *trans–gauche* (*tg*, $\chi \approx 180°$).[39] These three orientations were examined for every molecular model.

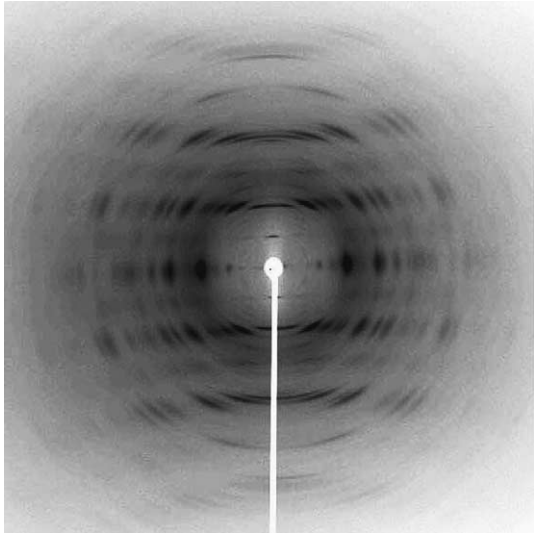

Figure 1. X-ray fiber diffraction pattern of chitosan/HI type I salt recorded on an Imaging Plate (*R*-AXIS IV^{++}, Rigaku) at BL40B2, SPring-8, Japan.

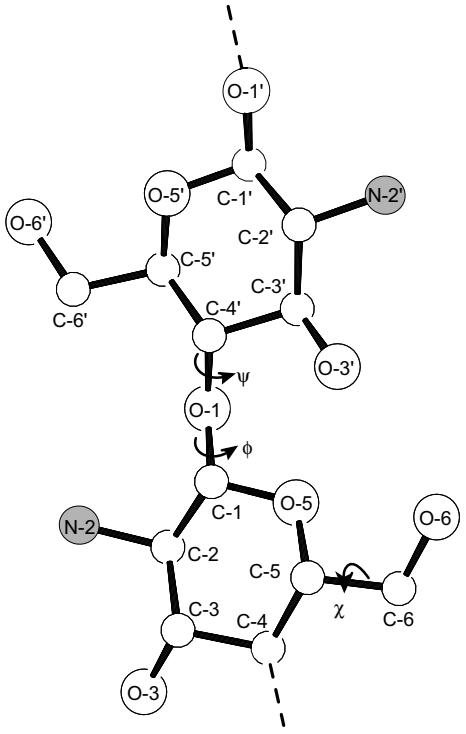

Figure 2. Molecular structure of chitosan/HI type I salt with two main chain conformational angles (ϕ, ψ). The O-6 orientation is defined by dihedral angle χ. Prime and unprimed atoms are related by the molecular 2/1-helical symmetry.

2.3. Molecular and crystal packing

2.3.1. Packing of iodide ions. Since the diffraction pattern mainly resulted from a scattering of iodide ions, the location of iodide ions could be indicated by the characteristic features of intensity distribution. The intensities of diffraction spots on even layer lines were stronger than those on odd layer lines. This implied that the iodide ions are arranged along the fiber (c) axis with a repeat of half of the fiber period (about 5 Å). Therefore, two independent iodide ions at 5-Å intervals along the c-axis are packed in the unit cell according to the symmetry of the space group $P2_1$. Positions of the iodide ions were searched in terms of the *R*-factors against all hkl reflections. Two independent iodide ions located at similar x- and y-positions but apart from each other

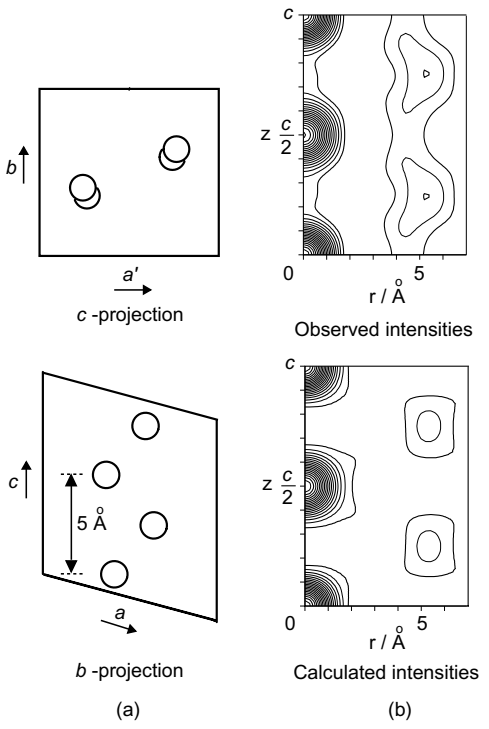

Figure 3. (a) Positions of iodide ions in a unit cell. (b) Cylindrical Patterson maps were generated by using the observed intensities of chitosan/HI type I salt (up) and the calculated intensities from iodide ions with positions shown in (a) (bottom).

about 5 Å along the z-direction were obtained (Fig. 3a). These locations could also be confirmed by the similarity between two cylindrical Patterson maps that were generated by using observed intensities and calculated intensities from the iodide ions packed as mentioned above (Fig. 3b). The peak at $r = 0$, $z = c/2$ corresponds to the vector peak between two independent iodide ions while the peak at $r = 5.5$, $z = c/4$ corresponds to that between iodide ions, which related by the crystallographic 2_1 symmetry.

2.3.2. Packing of chitosan chains. Two polymer chains were related by the crystallographic 2_1 symmetry along the b-axis. Therefore, the chains spontaneously align in up and down directions. Here, the corner chain in the unit cell is assumed to be oriented up. That is, the z-coordinate of O-5 in corner chain is larger than that of C-5 in the same chain. Molecular azimuthal angles, μ, were searched together with the (x, y) position in terms of the R-factor against the equatorial reflections. The orientation of the O-6 atom had not been taken into account at this stage. Locating polymer chain at $u = 0$, $v = 0$ with $\mu = 170°$ yields the minimum R-factor. Next, the translation along the fiber axis of polymer chains was searched with a step of 0.5 Å against the hkl reflections, and the nonbonded interatomic interaction was taken into account. Refinement of chain packing parameters resulted in nine models that are different in their z-positions. These models were subjected to a further step of refinement.

2.3.3. Determination of the O-6 orientation. Three orientations, *gg*, *gt*, *tg*, were determined for all nine models from the previous step ($9 \times 3 = 27$ models). After including O-6, the plausible chain locations along the z-direction were reduced to four ($4 \times 3 = 12$ models) because the z-position of the other five models shifted to one of the above four positions during refinement. Two out of four locations lower the R-factors by several percents. These two locations differed mainly in the z-position. The first has $w \approx 0$ and the other has $w \approx 0.5$. The *gt* orientation of both locations showed lower R-factors than the *gg* orientation. According to the data obtained, these two models could be considered as the same model. Here, the model with $w \approx 0$ was chosen to represent the structure of chitosan/HI type I salt. In the next step, the conformational parameters were refined together with the packing parameters. Final refined parameters are shown in Table 1. The fractional coordinates are shown in Table 2. Observed and calculated structure amplitudes are listed in Table 3.

3. Results and discussion

3.1. Comparison of the chitosan/HI salt with previous work[32]

3.1.1. Sample preparation. A mixture of type I and type II salt was obtained when the salt was prepared at room temperature for 20 min as previously reported.[32] Since

Table 1. Final refined parameters for the chitosan/HI type I salt

Torsion angles and bond angle at the glycosidic linkage/°	
ϕ(C-2–C-1–O-1–C-4′)	152.0
ψ(C-1–O-1–C-4′–C-3′)	87.6
τ(C-1–O-1–C-4′)	116.7
Orientation of the O-6 atom/°	
χ (O-5–C-5–C-6–O-6)	48.3
Packing parameters of chitosan chain and iodide ions	
Chitosan chain	
Azimuthal angle/° (μ1)	170.0
$u1$, $v1$, $w1$	−0.0023, 0.0031, 0.0045
Iodide ions	
I-1 ($u2, v2, w2$)	0.4116, 0.2415[a], 0.0994
I-2 ($u3, v3, w3$)	0.3530, 0.2532, 0.5933
Scale factor	5.03
Attenuation factor	20.7
R-factors (R/Rw)	
Excluded unobserved reflections	0.17/0.17
Included unobserved reflections	0.19/0.18

[a] The $v2$ value was fixed through the refinement.

Table 2. Fractional atomic coordinates of the asymmetric unit of chitosan/HI type I salt

Atom	*x*	*y*	*z*	Atom	*x*	*y*	*z*
O-1	−0.0513	0.0826	0.6089	O-1′	0.0467	−0.0764	1.1322
C-1	−0.0501	0.0110	0.4931	C-1′	0.0455	−0.0047	1.0159
O-5	0.0991	−0.0011	0.4889	O-5′	−0.1037	0.0073	0.9405
C-5	0.1139	−0.0743	0.3726	C-5′	−0.1185	0.0805	0.8172
C-6	0.2763	−0.0911	0.3868	C-6′	−0.2809	0.0973	0.7539
O-6	0.3513	−0.1406	0.5165	O-6′	−0.3559	0.1468	0.8478
C-2	−0.1347	0.0933	0.3727	C-2′	0.1301	−0.0871	0.9358
N-2	−0.2915	0.1052	0.3768	N-2′	0.2869	−0.0990	1.0148
C-3	−0.1235	0.0265	0.2428	C-3′	0.1189	−0.0203	0.8006
O-3	−0.1906	0.1124	0.1319	O-3′	0.1860	−0.1062	0.7218
C-4	0.0363	0.0025	0.2455	C-4′	−0.0409	0.0037	0.7271
H-1	−0.0933	−0.0826	0.4910	H-1′	0.0887	0.0888	1.0344
H-2	−0.0941	0.1881	0.3780	H-2′	0.0895	−0.1819	0.9218
H-3	−0.1768	−0.0627	0.2310	H-3′	0.1722	0.0689	0.8143
H-4	0.0856	0.0922	0.2419	H-4′	−0.0902	−0.0860	0.7000
H-5	0.0701	−0.1674	0.3715	H-5′	−0.0747	0.1736	0.8369
H-6a	0.2918	−0.1578	0.3184	H-6a′	−0.2963	0.1640	0.6781
H-6b	0.3183	−0.0003	0.3725	H-6b′	−0.3229	0.0065	0.7196
I-1	0.4116	0.2415	0.0994	I-2	0.3530	0.2532	0.5933

Table 3. Observed (F_o) and calculated (F_c) structure amplitudes of chitosan/HI type I salt[a]

Spot no.	*h*	*k*	*l*	F_c	F_o	Spot no.	*h*	*k*	*l*	F_c	F_o	Spot no.	*h*	*k*	*l*	F_c	F_o
1	1	0	0	18	18		−2	1	1	30	(19)		2	0	2		
2	1	1	0	67	46		−1	2	1	37	(19)		−3	0	2	234	284
3	0	2	0	63	54	14	1	2	1				2	1	2	22	(22)
4	2	0	0				2	0	1	65	75		−3	1	2	22	(22)
	1	2	0			15	2	1	1			25	0	3	2		
	2	1	0	452	493		−2	2	1	56	62		−1	3	2	164	108
	2	2	0	22	(22)		−3	0	1	8	(22)	26	2	2	2		
5	1	3	0			16	0	3	1				−3	2	2		
	3	0	0				−1	3	1				1	3	2		
	3	1	0	283	268		2	2	1				−2	3	2	148	135
6	2	3	0				−3	1	1	104	65	27	3	0	2		
	3	2	0	142	128		1	3	1	23	(23)		−4	0	2		
7	0	4	0	77	69	17	3	0	1				3	1	2		
8	1	4	0				−2	3	1				−4	1	2	72	74
	4	0	0	102	102		−3	2	1	78	52		2	3	2	29	(27)
9	3	3	0				3	1	1	15	(25)		0	4	2	31	(27)
	4	1	0	88	102		2	3	1	42	(26)		−3	3	2	30	(27)
10	2	4	0	49	86	18	0	4	1				−1	4	2	32	(27)
	4	2	0	60	(29)		3	2	1			28	3	2	2		
11	1	5	0				−4	0	1				1	4	2		
	3	4	0	62	59		−1	4	1	51	69		−4	2	2		
	4	3	0	7	(31)	19	0	0	2				−2	4	2	81	57
12	5	0	0				−1	0	2	84	74	29	2	4	2		
	2	5	0			20	0	1	2				3	3	2		
	5	1	0	73	89		−1	1	2	260	261		−3	4	2		
	0	0	1	8	(6)	21	1	0	2				4	0	2		
13	−1	0	1	24	16		−2	0	2	179	140		−4	3	2		
	0	1	1	5	(13)	22	1	1	2				−5	0	2	78	107
	−1	1	1	13	(14)		−2	1	2	105	99	30	4	1	2		
	1	0	1	2	(15)	23	0	2	2				−5	1	2		
	1	1	1	38	(16)		−1	2	2	98	86		0	5	2		
	−2	0	1	27	(17)	24	1	2	2				−1	5	2	79	59
	0	2	1	12	(18)		−2	2	2				0	0	3	13	(11)
31	−1	1	3	28	44	39	−1	2	4								
32	0	1	3				1	0	4	68	67						
	−2	0	3	29	45	40	−3	0	4								
33	−2	1	3	47	41		0	2	4								

Table 3 (*continued*)

Spot no.	*h*	*k*	*l*	F_c	F_o	Spot no.	*h*	*k*	*l*	F_c	F_o	Spot no.	*h*	*k*	*l*	F_c	F_o
	1	0	3	17	(18)		−2	2	4								
	−1	2	3	21	(19)		1	1	4								
	1	1	3	20	(19)		−3	1	4	135	156						
	0	2	3	18	(19)		1	2	4	6	(24)						
34	−2	2	3				−3	2	4	4	(24)						
	−3	0	3	42	57		−1	3	4	11	(24)						
	−3	1	3	47	(22)	41	0	3	4								
	1	2	3	43	(22)		2	0	4								
	2	0	3	26	(23)		−2	3	4								
35	−1	3	3				−4	0	4								
	0	3	3				2	1	4	71	71						
	2	1	3				−4	1	4	39	(26)						
	−3	2	3	48	51	42	1	3	4								
	−2	3	3	37	(25)		−3	3	4								
	−4	0	3	21	(26)		2	2	4	76	102						
	1	3	3	7	(26)	43	−4	2	4								
	2	2	3	19	(26)		−1	4	4	59	63						
	−4	1	3	13	(26)		0	4	4	17	(29)						
36	−3	3	3				0	0	5	1	(9)						
	−1	4	3				−2	1	5	10	(11)						
	3	0	3				0	1	5	9	(15)						
	0	4	3			44	−3	0	5								
	3	1	3				−1	2	5								
	−4	2	3	55	44		−3	1	5								
37	−1	1	4				−2	2	5	29	40						
	0	0	4														
	−2	0	4	74	63												
38	0	1	4														
	−2	1	4	101	135												

[a] F_o in the parentheses are those for unobserved reflections. These values are one half of the observational threshold.

there was a report[40] that different types of salts were obtained in some acids depending on the preparation conditions, we tried various conditions to obtain pure chitosan/HI type I salt. The specimen used in this study was finally obtained by immersing chitosan in 6 M HI aqueous solution at 4 °C for 24 h. However, we have found that only by these conditions, diffraction patterns of type II[35] or mixture of type I and type II could be occasionally obtained. This indicated that only the preparation temperature and time were not the key factor for taking different conformation for chitosan/HI salt.

3.1.2. Unit cell parameters. The monoclinic unit cell with cell dimensions of $a = 12.58$, $b = 14.88$, c (fiber axis) $= 10.45$ Å and $\gamma = 102.27°$ was reported in the previous work.[32] However, the monoclinic unit cell with the dimensions $a = 9.46(2)$, $b = 9.79(2)$ and c (fiber axis) $= 10.33(2)$ Å and $\beta = 105.1(2)°$ could be indexed in this study. In the previous work, 18 diffraction spots up to the fourth layer line were observed, while 44 diffraction spots up to the fifth layer line were observed in the present study. The higher quality of diffracted data and smaller volume of the unit cell obtained in this study suggested better reliability of the unit cell parameters.

3.2. Molecular structure

Polymer molecules in the chitosan/HI salt take an extended twofold helical symmetry with a repeating period of 10.33 Å. The molecular structure was stabilized by O-3···O-5 intramolecular hydrogen bonds (2.55 Å). The main chain conformation angles, ϕ(C-2–C-1–O-1–C-4′) and ψ(C-1–O-1–C-4′–C-3′), were 152.0° and 87.6°, respectively. The glycosidic linkage angle τ(C-1–O-1–C-4′) was 116.7°. The O-6 atom approached the *gt* conformation, χ(O-5–C-5–C-6–O-6) = 48.3°. The polysaccharide conformation in the salt was very similar to those in anhydrous[25] and hydrated chitosan.[24] This indicates that in the present case, the salt formation did not affect the main-chain conformation.

3.3. Crystal structure

Two adjacent chains aligned in a zigzag pattern along the *b*-axis are related to each other by the crystallographic 2_1 symmetry along this direction (Fig. 4). The

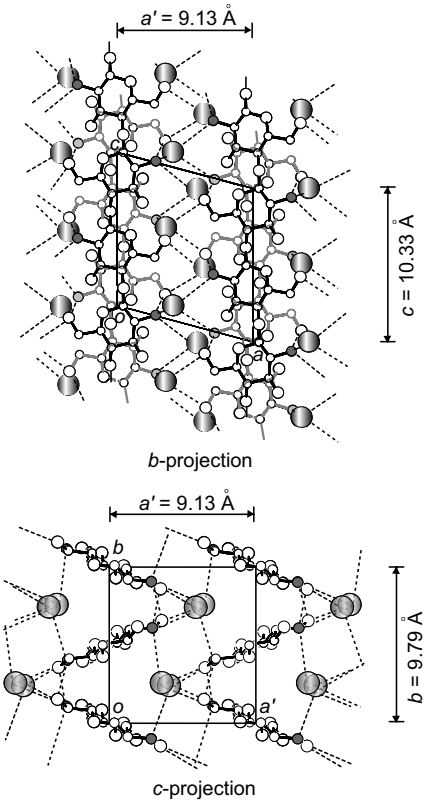

Figure 4. The packing structure of chitosan/HI type I salt is projected along *b*- and *c*-axes. Dashed lines represent hydrogen bonds. Grey circles represent N atoms and gradient shaded circles represent I^- ions.

corner chain was assumed to be oriented 'up', and, therefore, another chain at the center of the *b*-direction was spontaneously oriented 'down'. These polymer chains are linked to each other along the *b*-axis by two N-2···O-6 hydrogen bonds (2.84 and 2.85 Å). These zigzag sheets piled up along the *a*-direction.

In the unit cell, two independent iodide ions made a columnar structure with 5-Å intervals along the *c*-axis. There was another column of iodide ions that was related to the first one by the crystallographic 2_1 symmetry along the *b*-axis. These columns are located at the bending points of the zigzag sheets of polymers (Fig. 4).

3.4. Nonbonded interatomic interaction

The extended 2/1-helical conformation was stabilized by typical O-3···O-5 intramolecular hydrogen bonds (2.55 Å). Two N-2···O-6 hydrogen bonds (2.84 and 2.85 Å) connected adjacent chitosan chains along the *b*-direction. No direct interaction between the chains along the *a*-direction was found. The N-2 atoms were hydrogen donors to the O-6 atom and two iodide ions (Table 4). This implied that NH_3^+ occurred in the structure. The O-6 atoms donated hydrogen to an iodide ion.

Two independent iodide ions were stabilized in the salt structure by an electrostatic interaction with N-2 atoms and by forming hydrogen bonds to N-2 atoms and O-6 atoms of the chains. Each iodide ion coordinated with the other three atoms. That is, one iodide ion accepted three H atoms from N-2, and another iodide ion accepted one H atom from N-2 and two H atoms from O-6 (Fig. 4, Table 4).

The interaction between polymer chains and iodide ions are of the type N-2···I^- and O-6···I^- hydrogen bonds. According to the Cambridge Structure Database (CSD),[41] the N···I^- distance and C–N···I^- angle were 3.41–3.81 Å and 82.9–137.4°, respectively. The average values of those distances and angles were 3.59 Å and 107.4°, respectively. In this study, the N-2···I^- distances and C-2–N-2···I^- angles were 3.52–3.71 Å and 96.56–126.35°, respectively. The O-6···I^- distances and the C-6–O-6···I^- angles were 3.43, 3.44 Å and 91.61°, 92.62° while those distances and angles from CSD were 3.38–3.66 Å and 91.3–133.7°, respectively. The average of those distances and angles from the database were 3.50 Å and 109.3°, respectively.

3.5. Speculation of the salt formation mechanism

The unit cell parameters and number of polymer chains running through the unit cell of the chitosan/HI salt were very similar to those of the hydrated chitosan if two adjacent unit cells of the salt were considered to be a new unit cell. Two plausible conversion processes from hydrated chitosan to the salt were proposed (Fig. 5, left

Table 4. Details of hydrogen bonds among chains and iodide ions

Donor, D	Acceptor, A[a]	$d(D\cdots A)$/Å	Precursor, *P*	$\angle(P-D\cdots A)$/°
N-2	O-6$^{(i)}$	2.84	C-2	112.14
N-2′	O-6′$^{(i)}$	2.85	C-2	113.71
N-2	I-1$^{(ii)}$	3.70	C-2	124.23
N-2′	I-1$^{(iii)}$	3.56	C-2	106.22
N-2	I-2$^{(iv)}$	3.52	C-2	96.56
N-2′	I-1$^{(v)}$	3.71	C-2	126.35
O-6	I-2$^{(vi)}$	3.44	C-6	92.62
O-6′	I-2$^{(vii)}$	3.43	C-6	91.61

[a] Symmetry codes: (i) $-x, 0.5+y, -1-z$; (ii) $-1+x, y, z$; (iii) $x, y, 1+z$; (iv) $-x, -0.5+y, 1-z$; (v) $1-x, -0.5+y, 1-z$; (vi) $1-x, -0.5+y, 1-z$; (vii) $-1+x, y, z$.

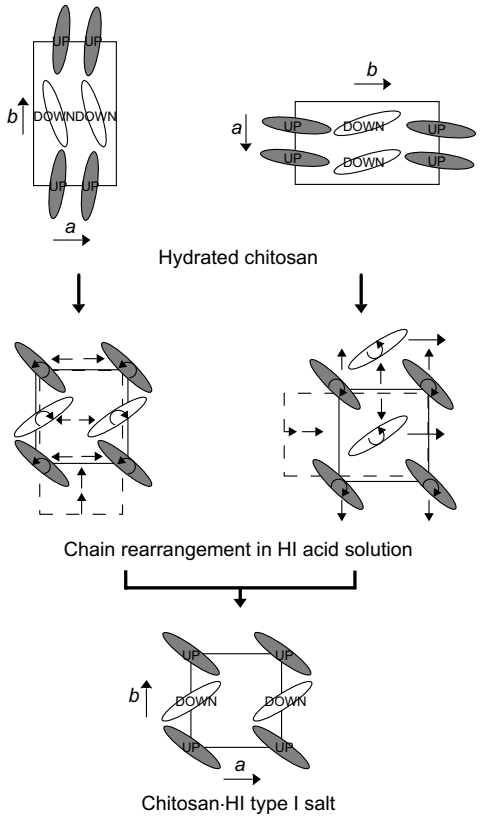

Figure 5. Plausible mechanism of chain rearrangement during conversion process from hydrated chitosan to chitosan/HI type I salt. Shaded ellipsoids denote up-pointing molecules.

and right pathways). To produce an easy-to-understand illustration, the hydrated chitosan was turned in different directions (Fig. 5, up left and right). In the acid solution, hydrogen bonds in the hydrated chitosan crystal were broken, allowing the polymer chains to move. The up-and-down-pointing sheets rotated in opposite direction for the first pathway (Fig. 5, middle left). The up-and-down-pointing chains rotated in opposite directions together with the down-pointing chains intervening between the up-pointing chains for the second pathway (Fig. 5, middle right). The *a*-extension and *b*-shrinkage, together with each of those chain rearrangements, led to an alternate up-and-down layer structure along the *b*-axis of the salt structure. At the same time, $-NH_3^+$ and I^- interaction had occurred. Since the salt could be transformed from hydrated rather than anhydrous crystalline forms, and the relation between iodide columns and polymer chains in the salt structure was similar to that of water columns and polymer chains in the hydrated crystalline form, water molecules were believed to be replaced by these iodide ions when the salt was formed. The salt was stabilized by hydrogen bonds between these iodide ions and the polymer chains, together with the electrostatic interaction.

3.6. Conclusions

A detailed structure of chitosan/HI type I salt is proposed. The polymer chains adopt an extended 2/1 helical conformation with glycosidic angles, $\phi = 152.0°$, and $\psi = 87.6°$. The orientation of the O-6 atom approximates the *gt* conformation ($\chi = 48.3°$), which is similar to those of anhydrous and hydrated chitosan. The glycosidic linkage angle τ was 116.7°. The molecular structure was stabilized by strong O-3···O-5 hydrogen bonds (2.55 Å). Two adjacent chains having a zigzag arrangement along the *b*-axis are related to each other by the crystallographic 2_1 symmetry along this direction. The adjacent chains are connected to each other by two N-2···O-6 hydrogen bonds (2.84 and 2.85 Å) along the *b*-direction. As a result, zigzag sheets that pile up along the *a*-axis are formed. Two independent iodide ions are arranged at 5-Å intervals along the fiber axis. In the unit cell, two columns of iodide ions are packed at the bending points of the zigzag sheets of the chitosan chains. The interactions between the chain and iodide ions are N-2···I^- (3.52-3.71 Å) and O-6···I^- (3.43, 3.44 Å) hydrogen bonds. The salt is stabilized by those hydrogen bonds and the electrostatic interaction between $-NH_3^+$ and I^- species. Iodide ions are speculated to replace water molecules in the hydrated crystalline form when the salt is formed.

4. Experimental section

4.1. Materials

Chitosan was produced from the tendon of *Chionoecetes opilio* O. Fabricius crab by deacetylation with 50% sodium hydroxide solution at 110 °C for 2 h under nitrogen atmosphere. The degree of N-acetylation was determined by colloidal titration, and the viscosity-average degree of polymerization of the obtained chitosan was found to be almost 0% and at least 10,800, respectively.[42]

Chitosan/HI salt was prepared following the conditions reported by Ogawa and co-workers.[32] The tendon chitosan was immersed in aq 6 M HI solution at room temperature (rt) for 20 min. The X-ray fiber diffraction pattern showed that the specimen was a mixture between type I and type II. To obtain the pure type I salt form, the preparation conditions were adjusted. The salt was prepared by varying the preparation conditions as follows: rt, 20 min; rt, 24 h; 4 °C, 20 min; 4 °C, 24 h. The salt was washed in 2-propanol and 75% 2-propanol. The specimen was dried in air before the X-ray measurement. Chitosan/HI type I salt used in this study was obtained by immersing chitosan in aq 6 M HI solution at 4 °C for 24 h. The density of the specimen was measured by the flotation method.

4.2. X-ray measurement and data correction

The specimen was exposed to the synchrotron radiation ($\lambda = 1.00$ Å) at BL40B2, SPring-8, for 3 min. The diffraction pattern was recorded on an Imaging Plate (*R*-AXIS IV^{++}, Rigaku). The camera length (133 mm) was calibrated using the characteristic *d*-spacings of silicon. X-ray intensity (I_o) of each diffraction spot and unit cell parameters were determined using the in-house data processing software.[24,43,44] The measured intensities (I_o) were corrected for the Lorentz and polarization factors. The absorption effect was corrected in this study.

4.3. Linked-atom least-squares analysis

At each stage of establishing molecular and packing models and refinement, the quantity Ω was minimized.

$$\Omega = \sum_m w_m(|F_m^o| - |F_m^c|)^2 + \sum_i k_i(d_i - d_i^o)^2 + \sum_j e_j(p_j - p_j^o)^2 + \sum_q \lambda_q G_q.$$

The first term ensures the optimum agreement between observed (F_o) and calculated (F_c) structure amplitudes. The unobserved reflections with longer spacings than that of the outermost reflection on the same layer line were also included in the structural analysis and assumed to have half of the intensity of the observational threshold. The weight of the reflection, w_m, was fixed to 1.0 for all observed reflections. For the unobserved reflections, $w_m = 1.0$ when $|F_m^c| \geqslant |F_m^o|$ and $w_m = 0$ when $|F_m^c| < |F_m^o|$. The second term ensures the optimization of noncovalent interatomic interactions. The third term is used to restrain certain parameters or quantities, such as torsional angles, bond angles or interatomic distances to their expected values. The last term is used to impose constraints we have chosen.

The agreement between observed and calculated structure amplitudes is described in terms of the *R*-factors, which were defined by

$$R \text{ (Normal)} = \frac{\sum ||F_o| - |F_c||}{\sum |F_o|},$$

$$Rw \text{ (Quadratic weighted)} = \left[\frac{\sum w(|F_o| - |F_c|)^2}{\sum wF_o^2}\right]^{1/2}.$$

Atomic scattering factors for calculating structure factors were obtained by using the method and values given in the literature.[45] Computations were carried out on a PC using the WINLALS[37] program version 1.105.

Acknowledgements

The synchrotron radiation experiments were performed at BL40B2 in SPring-8 with the approval of the Japan Synchrotron Radiation Research Institute (JASRI). This research was partially supported by a Grant-in-Aid for Young Scientists (B) (15750098) from the Japan Society for the Promotion of Science (JSPS). A.L. thanks the Ministry of Education, Culture, Sports, Science and Technology (MEXT) for financial support.

References

1. Molinaro, G.; Leroux, J. C.; Damas, J.; Adam, A. *Biomaterials* **2002**, *23*, 2717–2722.
2. VandeVord, P. J.; Matthew, H. W.; DeSilva, S. P.; Mayton, L.; Wu, B.; Wooley, P. H. *J. Biomed. Mater. Res.* **2002**, *59*, 585–590.
3. Molinaro, G.; Leroux, J. C.; Damas, J.; Adam, A. *Biomaterials* **2002**, *23*, 2717–2722.
4. Rao, S. B.; Sharma, C. P. *J. Biomed. Mater. Res.* **1997**, *34*, 21–28.
5. Koping-Hoggard, M.; Tubulekas, I.; Guan, H.; Edwards, K.; Nilsson, M.; Varum, K. M.; Artursson, P. *Gene Ther.* **2001**, *8*, 1108–1121.
6. No, H. K.; Lee, S. H.; Park, N. Y.; Meyers, S. P. *J. Agric. Food Chem.* **2003**, *51*, 7659–7663.
7. Chung, Y. C.; Wang, H. L.; Chen, Y. M.; Li, S. L. *Bioresour. Technol.* **2003**, *88*, 179–184.
8. Koide, S. S. *Nutr. Res.* **1998**, *18*, 1091–1101.
9. Roller, S.; Covill, N. *Int. J. Food Microbiol.* **1999**, *47*, 67–77.
10. Park, R.; Jo, K.; Jo, Y.; Jin, Y.; Kim, K.; Shim, J.; Kim, Y. *J. Microbiol. Biotechnol.* **2002**, *12*, 84–88.
11. Avital, M. B.; Jessica, L. C.; Elias, K. M.; Jack, D. S. *Int. J. Antimicrob. Agents* **2003**, *22*, 168–171.
12. Qin, C.; Du, Y.; Xiao, L.; Li, Z.; Gao, X. *Int. J. Biol. Macromol.* **2002**, *31*, 111–117.
13. Qin, C.; Zhou, B.; Zeng, L.; Zhang, Z.; Liu, Y.; Du, Y.; Xiao, L. *Food Chem.* **2003**, *84*, 107–115.
14. Hasegawa, M.; Yagi, K.; Iwakawa, S.; Hirai, M. *Jpn. J. Cancer Res.* **2001**, *92*, 459–466.
15. Muzzarelli, R. A. A. *Natural Chelating Polymers: Algenic Acid, Chitin and Chitosan*; Pergamon: Oxford, 1973; pp 145–176.
16. Domard, A.; Piron, E. *Adv. Chitin Sci.* **2000**, *4*, 295–301.
17. Vold, I. M. N.; Vårum, K. M.; Guibal, E.; Smidsrød, O. *Carbohydr. Polym.* **2003**, *54*, 471–477.
18. Ebihara, K.; Schneeman, B. O. *J. Nutr.* **1989**, *119*, 1100–1106.
19. Gallaher, D. D.; Gallaher, C. M.; Mahrt, G. J.; Carr, T. P.; Hollingshead, C. H.; Hesslink, R. J.; Wise, J. *J. Am. Col. Nutr.* **2002**, *21*, 428–433.
20. Castro, I. A.; Tirapegui, J.; Benedicto, M. L. *Food Chem.* **2002**, *80*, 323–330.
21. Bokura, H.; Kobayashi, S. *Eur. J. Clin. Nutr.* **2003**, *57*, 721–725.
22. Ishihara, M.; Ono, K.; Sato, M.; Nakanishi, K.; Saito, Y.; Yura, H.; Matsui, T.; Hattori, H.; Fujita, M.; Kikuchi, M.; Kurita, A. *Wound Repair Regen.* **2001**, *9*, 513–521.
23. Shen, E.; Fu, E.; Hsieh, Y. *Adv. Chitin Sci.* **1998**, *3*, 284–290.

24. Okuyama, K.; Noguchi, K.; Miyazawa, T.; Yui, T.; Ogawa, K. *Macromolecules* **1997**, *30*, 5849–5855.
25. Okuyama, K.; Noguchi, K.; Hanafusa, Y.; Osawa, K.; Ogawa, K. *Int. J. Biol. Macromol.* **1999**, *26*, 285–293.
26. Okuyama, K.; Noguchi, K.; Kanenari, M.; Egawa, T.; Osawa, K.; Ogawa, K. *Carbohydr. Polym.* **2000**, *41*, 237–247.
27. Mazeau, K.; Winter, W. T.; Chanzy, H. *Macromolecules* **1994**, *27*, 7606–7612.
28. Ogawa, K.; Hirano, S.; Miyanishi, T.; Yui, T.; Watanabe, T. *Macromolecules* **1984**, *17*, 973–975.
29. Kawada, J.; Abe, Y.; Yui, T.; Okuyama, K.; Ogawa, K. *J. Carbohydr. Chem.* **1999**, *18*, 559–571.
30. Gardner, K. H.; Blackwell, J. *Biopolymers* **1975**, *14*, 1581–1595.
31. Gardner, K. H.; Blackwell, J. *Biopolymers* **1974**, *13*, 1975–2001.
32. Ogawa, K.; Inukai, S. *Carbohydr. Res.* **1987**, *160*, 425–433.
33. Ogawa, K.; Nakata, K.; Yamamoto, A.; Nitta, Y. *Chem. Mater.* **1996**, *8*, 2349–2351.
34. Okuyama, K.; Osawa, K.; Hanafusa, Y.; Noguchi, K.; Ogawa, K. *J. Carbohydr. Chem.* **2000**, *19*, 789–794.
35. Lertworasirikul, A.; Tsue, S.; Noguchi, K.; Okuyama, K.; Ogawa, K. *Carbohydr. Res.* **2003**, *338*, 1229–1233.
36. Kawahara, M.; Yui, T.; Oka, K.; Zugenmaier, P.; Suzuki, S.; Kitamura, S.; Okuyama, K.; Ogawa, K. *Biosci. Biotechnol. Biochem.* **2003**, *67*, 1545–1550.
37. Okada, K.; Noguchi, K.; Okuyama, K.; Arnott, S. *Comput. Biol. Chem.* **2003**, *27*, 265–285.
38. Arnott, S.; Scott, W. E. *J. Chem. Soc., Perkin Trans. 2* **1972**, 324–335.
39. Sundaralingam, M. *Biopolymers* **1968**, *6*, 189–213.
40. Kawada, J.; Yui, T.; Abe, Y.; Ogawa, K. *Biosci. Biotechnol. Biochem.* **1998**, *62*, 700–704.
41. Allen, F. H.; Bellard, S.; Brice, M. D.; Cartwright, B. A.; Doubleday, A.; Higgs, H.; Hummelink, T.; Hummelink-Peters, B. G.; Kennard, O.; Motherwell, W. D. S.; Rodgers, J. R.; Watson, D. G. *Acta Crystallogr.* **1979**, *B35*, 2331–2339.
42. Ogawa, K. *Agric. Biol. Chem.* **1991**, *55*, 2375–2379.
43. Obata, Y.; Okuyama, K. *Kobunshi Ronbunshu* **1994**, *51*, 371–378, *Chem. Abstr.* **1994**, *121*, 85552.
44. Okuyama, K.; Obata, Y.; Noguchi, K.; Kusaba, T.; Ito, Y.; Ohno, S. *Biopolymers* **1996**, *38*, 557–566.
45. Ibers, J. A., Hamilton, W. C., Eds.; *International Tables for Crystallography*; Kynoch: Birmingham, England, 1974, 4, pp 71–147.